

PHYSICAL REVIEW D

PARTICLES AND FIELDS

THIRD SERIES, VOLUME 32, NUMBER 3

1 AUGUST 1985

Opposite-sign dilepton production in ν_μ interactions

N. J. Baker, A.-M. Cnops,* P. L. Connolly,[†] S. A. Kahn, H. G. Kirk, M. J. Murtagh,
R. B. Palmer, N. P. Samios, and M. Tanaka
Brookhaven National Laboratory, Upton, New York 11973

C. Baltay, M. Bregman, D. Caroumbalis, L. D. Chen, H. French,[†] M. Hibbs, R. Hylton, M. Kalelkar,[§]
J. T. Liu, J. Okamitsu, G. Ormazabal, A. C. Schaffer, K. Shastri, and J. Spitzer**
Columbia University, New York, New York 10027

(Received 5 June 1984; revised manuscript received 6 February 1985)

We report on a high-statistics bubble-chamber experiment using the Fermilab 15-ft bubble chamber filled with a heavy neon/hydrogen mixture exposed to a wide-band neutrino beam. In a sample of 106 000 ν_μ interactions 249 events with a positron ($P_{e^+} > 0.3$ GeV/c) and a negative muon were observed. After corrections, the rate for opposite-sign dilepton production for ν_μ charged-current events is $(0.52 \pm 0.09)\%$. The E_ν dependence of this rate from threshold to ≈ 200 GeV is presented. The kinematic distributions and strange-particle content of the dilepton events are consistent with those expected from charm-particle production in neutrino interactions. A total of 58 neutral strange particles ($\Lambda \rightarrow p\pi^-$, $K_S^0 \rightarrow \pi^+\pi^-$) are observed in these events, where less than 16 are expected from conventional charged-current interactions. The presence of a significant excess of Λ 's is evidence for substantial charmed-baryon production.

I. INTRODUCTION

The observation of opposite-sign dilepton events in neutrino interactions was first reported¹ in 1975. Since then other counter experiments²⁻⁷ and a number of bubble-chamber experiments⁸⁻¹⁹ have reported similar events. The present data are consistent with the semileptonic decay of charmed particles produced in accordance with the Glashow-Iliopoulos-Maiani (GIM) mechanism.²⁰ However, little detailed information is actually available on charm production in neutrino interaction. This is in part due to the high-momentum cuts on the leptons and the lack of specific final-state information in counter experiments. Bubble-chamber experiments suffer from lack of statistics but have detailed final-state information.

We report here on the results of a relatively-high-statistics bubble-chamber experiment.²¹ A total of 249 opposite-sign dileptons (μ^-e^+) were obtained in the analysis of 132 000 pictures of neutrino interactions in a heavy Ne/H₂ mixture. There are essentially no momentum cuts on the tracks. Consequently, the dilepton rate as a function of energy is a measurement of the charm-production cross section in neutrino interactions. The strange-particle content of these events is consistent with that expected in the GIM model. There is a clear excess of both K^0 's and Λ 's compared to the number one would expect in normal charged-current interactions. This significant Λ excess indicates the production of charmed baryons. One of the dilepton events has an e^+ which

clearly does not extrapolate directly back to the primary vertex.²² This event is an example of a charm particle which decays after traveling an observable distance (≈ 1 cm) in the bubble chamber. The limits on the charm lifetime obtained from this observation are quite consistent with more recent determinations of the lifetimes in emulsion experiments or e^+e^- collisions.

In Sec. II the beam and detector are described. Details on the scanning and selection of dilepton candidates are discussed in Sec. III. Possible background sources of dilepton events are evaluated in Sec. IV. A detailed analysis of the μ^-e^+ events is presented in Sec. V. Various parameters of these events and kinematic quantities are discussed and the production rate is calculated. The strange-particle content of the events is explored and effective-mass distributions are examined for the presence of resonances in the charm-particle decays. Finally, the new information on charm production provided by this experiment is summarized in Sec. VI.

II. EXPERIMENTAL PARAMETERS

The experiment was performed in the Fermilab 15-ft bubble chamber filled with a heavy Ne/H₂ mixture (64% atomic neon by volume). The radiation length in the liquid is 40 cm and this provides excellent electron identification. The interaction length is 125 cm. Most hadrons will interact in the chamber while muons leave the chamber without interacting.

The beam used was the double-horn-focused wide-band neutrino beam. This is the most intense neutrino beam at Fermilab. The spectrum peaks at ≈ 30 GeV and extends from threshold to ≈ 200 GeV. For neutrino production the horn is set to focus positive mesons (π^+, K^+). Since mesons with negative charge are defocused by the horn, the contamination of other neutrino types in the beam is relatively small. The calculated relative event rates for the major neutrino types in the beam are

$$\nu_\mu : \bar{\nu}_\mu : \nu_e : \bar{\nu}_e = 100 : 3 : 1 : 0.1.$$

A total of 132 000 pictures was taken in three runs of approximately equal length. The average number of protons per pulse on target in each of the three runs was 0.8×10^{12} , 1.5×10^{12} , 1.3×10^{12} , a total of 1.5×10^{17} protons on target. The estimated number of candidate charged-current events in the film is 106 000.

III. DATA SELECTION

The film was scanned for events with an electron or positron candidate coming from the primary vertex. A minimum ionizing track was identified on the scan table as an e^\pm candidate if it spiraled or had bremsstrahlung with a visible $\gamma \rightarrow e^+e^-$ conversion. The selected events were measured and reconstructed by the program TVGP. The events were then examined by physicists to verify the e^\pm identification, to determine whether the measured charged tracks interacted or left the chamber without interaction, and to search for any additional components of the events such as V^0 candidates, γ conversions, or neutron interactions which were missed on the original scan. Only events where the e^\pm was identified by at least two signatures and had a momentum greater than 300 MeV/c were retained for further analysis.

The requirement of two signatures greatly reduces the probability that hadron tracks will accidentally be identified as e^\pm tracks. On the other hand, most genuine e^\pm 's will yield two signatures. This e^\pm detection efficiency was determined by examining converted photons in the chamber. The detection efficiency above 300 MeV/c is on average greater than 80% and for tracks above 1 GeV/c is close to unity. The 300-MeV/c cut was imposed to reduce the background from asymmetric Dalitz pairs as is discussed below.

An event was identified as a ν_μ charged-current event if it had a negative track which left the chamber without interacting. If there was more than one leaving negative track, the fastest was identified as the muon candidate. The calculation of the background from fake charged-current events due to noninteracting hadrons is discussed below. The final event sample contained 321 events with an e^+ candidate, of which 249 also had a muon candidate.

The scanning efficiency was determined from a rescan of 50% of the film to be $(75 \pm 5)\%$.

The total number of charged-current events in the film was determined by measuring all events on approximately 2% of the frames selected uniformly throughout the film. This normalization sample contains 2000 events. All visible neutral energy (V^0, γ, n) in these events was measured

and in the analysis the e^\pm and normalization samples were handled in a similar manner.

From an examination of the normalization frames it was determined that $(10 \pm 5)\%$ of the events were confused to the point where one could not identify an e^\pm track if it were present. The major source of the confusion was hadronic interactions or the presence of high-energy electromagnetic showers (presumably from photon conversions) very close to the vertex.

IV. BACKGROUNDS

The major background sources for μ^-e^+ events are $\bar{\nu}_e$ interactions where a π^- leaves the chamber without interacting, $\bar{\nu}_e \text{Ne} \rightarrow e^+\pi^- \dots$, and ν_μ charged-current events with an asymmetric Dalitz pair in which the e^- track is too low in energy to be visible.²³ Other backgrounds such as leptonic decays of hadrons near the vertex or accidental electromagnetic signatures on hadron tracks are negligible.

The background due to fake μ^- (π^- punchthrough) is obtained from a comparison of interacting and noninteracting tracks of both signs. This calculation is made using the complete e^+ event sample.

On the average, leaving tracks travel $\frac{4}{3}$ interaction lengths so 75% of all hadrons should interact. However, this number is strongly momentum dependent. The interaction probability for hadrons as a function of momentum is determined as the ratio of noninteracting to interacting positive tracks (excluding recoil protons). The actual ratios used were determined from a neutrino narrow-band exposure in the identical liquid because the statistics are better and potential problems from antineutrino contamination are significantly reduced. The resulting numbers are consistent with those determined using the present data. From the observed number of interacting negative tracks, the expected number of noninteracting negative mesons of a given momentum can be calculated. The number of real muons is obtained by subtracting the calculated number of leaving hadrons from the number of observed leaving negative tracks in that momentum region. For the sample of events containing an e^+ , the calculated average background from π^- punchthrough is $(13 \pm 5)\%$. The probability, for the sample of events containing an e^+ , that the leaving negative particle selected as the muon candidate is a good muon is shown in Fig. 1(a). Within statistics this probability is independent of the event energy. This is not surprising since the background source is $\bar{\nu}_e$ interactions which have a similar energy spectrum to ν_μ interactions. The same is not true for the charged-current-normalization data sample [Fig. 1(b)]. The predominant background source here is low-energy neutron and neutral-current interactions. Consequently, while the average π^- punchthrough is $(20 \pm 3)\%$, this is strongly dependent on the energy of the event varying from 28% at low energies to a few percent above 100 GeV.

The μ^-e^+ background due to asymmetric Dalitz pairs has been experimentally determined to be $(4.4 \pm 2.5)\%$. Here a Dalitz pair signifies either a true Dalitz pair or an external $\gamma \rightarrow e^+e^-$ conversion which on the scanning

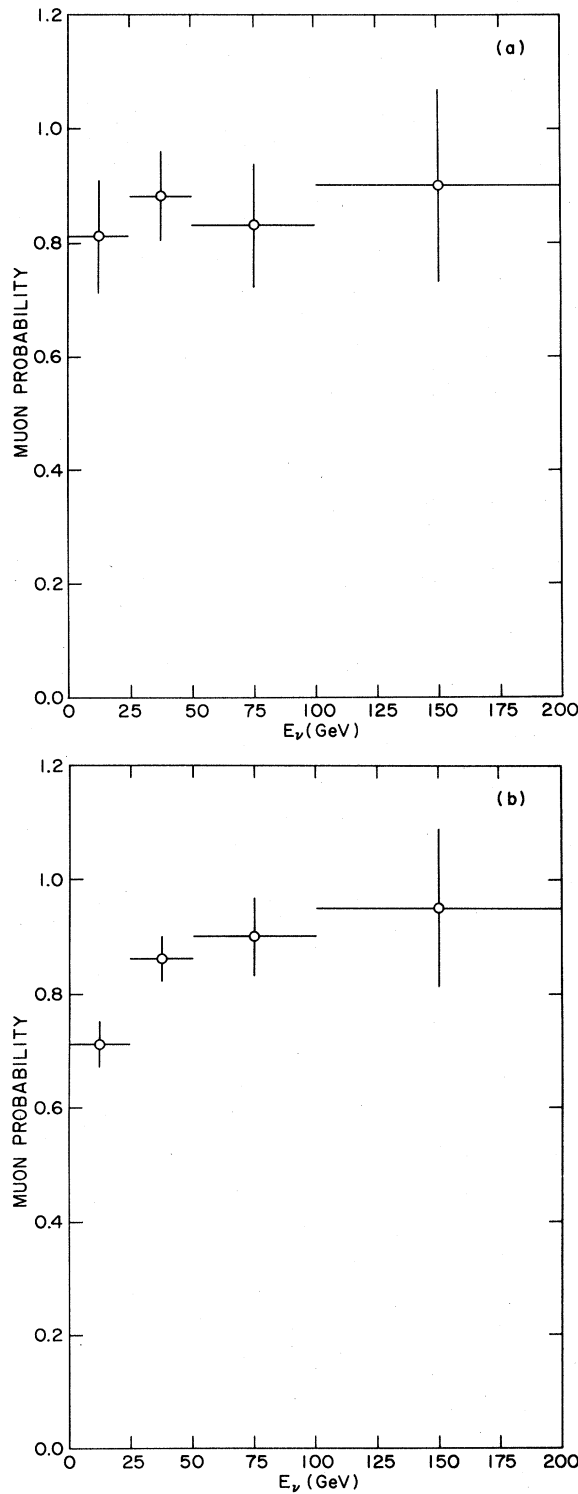


FIG. 1. Muon probability (probability that the leaving negative particle selected as the muon is a genuine muon) for (a) events containing an e^+ ; and (b) normalization events, as a function of the corrected neutrino energy.

table appears to originate at the vertex. The observed rate for such Dalitz pairs with an energy greater than 300 MeV/c is 4.2%. In addition, from a study of converted

γ 's the probability that an e^+e^- pair has a e^+ satisfying our selection criteria and does not have a visible e^- was measured to be 0.3%. Consequently 2.6×10^{-5} of the charged-current sample will have an asymmetric Dalitz pair where the e^- is not visible and the e^+ passes the selection criteria. This corresponds to 8 charged-current events or 4.4% of the μ^-e^+ sample.

A similar result can be obtained by a direct calculation. If one assumes that the π^0 momentum spectrum is the same as in the π^+ spectrum and that there are on average $2\pi^0$ per event, it is straightforward to calculate the expected number of asymmetric Dalitz pairs and the number of close conversions which appear to originate at the vertex. In this calculation it is assumed that e^- tracks with momentum greater than 5 MeV/c are visible and that on average conversions more than 0.5 cm from the vertex are separable. The resultant spectrum is shown in Fig. 2. The rate for asymmetric Dalitz pairs with a track of momentum greater than 300 MeV/c is 14.7×10^{-5} per charged-current event in good agreement with the measured value of 12.6×10^{-5} .

The total background in the μ^-e^+ sample is $(17 \pm 6)\%$. Since the dominant background is π^- punchthrough from $\bar{\nu}_e$ events one can directly calculate the background contribution to any distribution. From the ratio of leaving to interacting tracks one can determine the probability that a leaving negative track of a given momentum is a genuine muon. Each event with a muon candidate is then assigned an appropriate weight and the corrected kinematic distributions are generated.

V. OPPOSITE-SIGN DILEPTONS

A. Kinematic distributions

The positron momentum and muon momentum distributions for the μ^-e^+ events are shown in Figs. 3(a) and

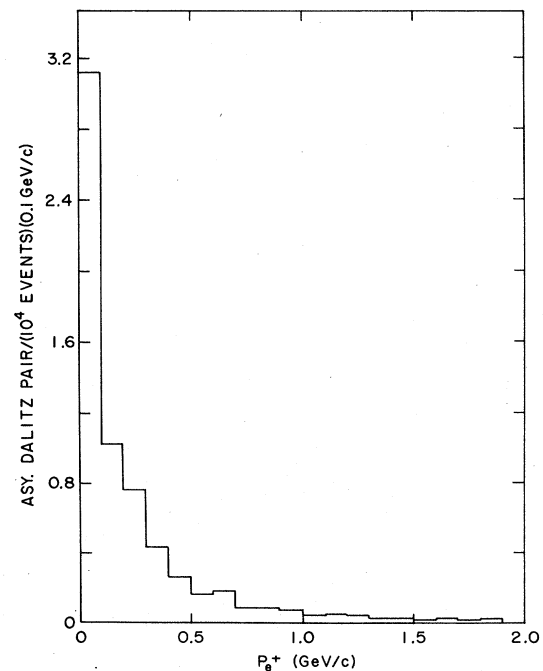


FIG. 2. Momentum spectrum for positrons from asymmetric Dalitz pairs and close photon conversions.

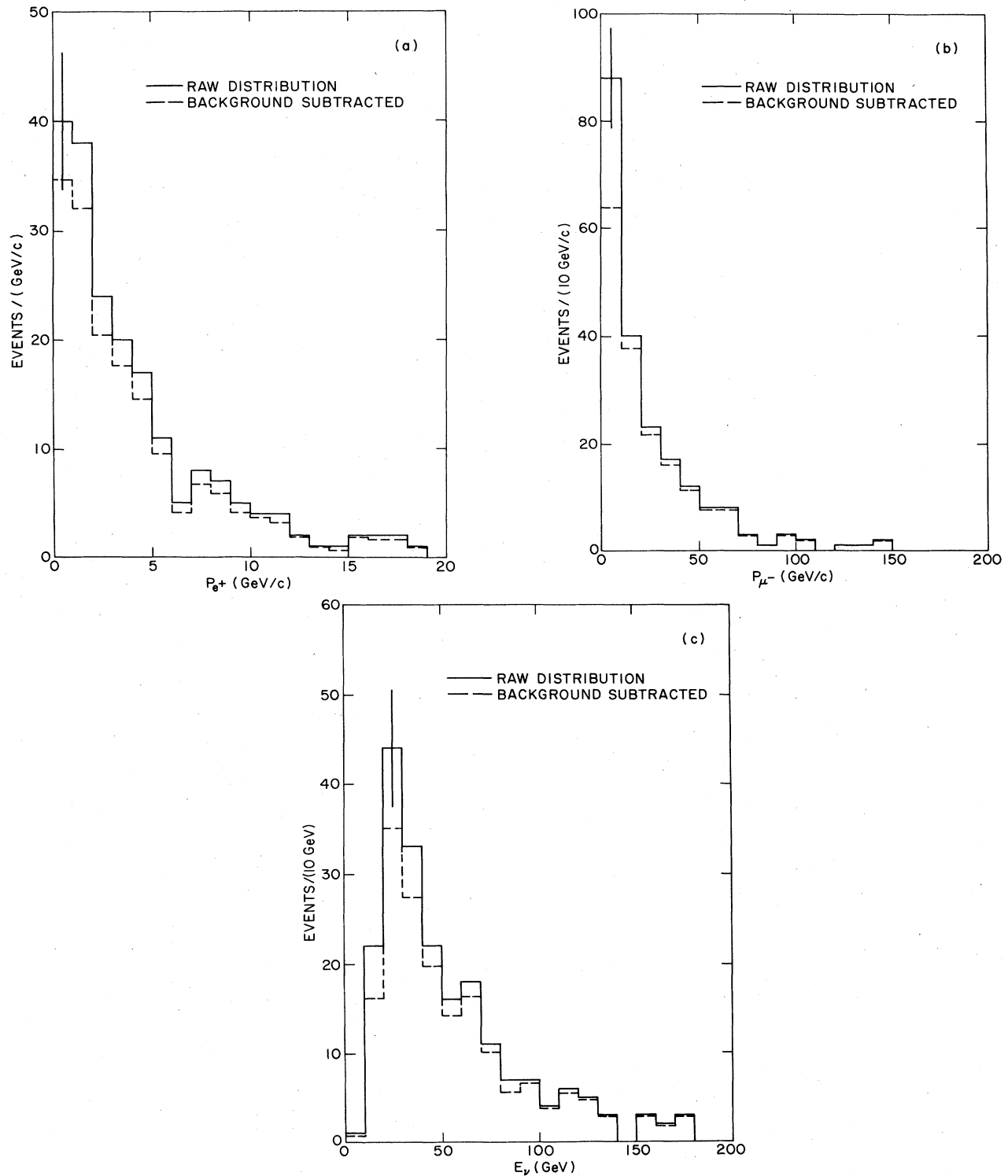


FIG. 3. Raw and corrected momentum spectra for (a) positions, (b) muons, and (c) incident neutrinos. The solid curve displays the raw distribution and the dashed curve is the background-subtracted distribution after weighting the muon momentum by the probability that it is genuine.

3(b), respectively. The electron momentum is obtained by a curvature measurement except in a few events where there is obvious early severe bremsstrahlung loss. In these cases the converted $\gamma \rightarrow e^+e^-$ energies from the brems-

strahlung are included in the electron momentum.

The visible energy E_{vis} comprises all charged and converted neutral energy (π^0 's, neutrons, etc.) which is judged to be associated with the primary vertex ($\gamma \rightarrow e^+e^-$ con-

versions which do not point to the primary vertex or are tangent to the e^+ track are not included). To reduce the effects of missing neutral particles in calculating the kinematic variables a corrected neutrino energy (E_ν) was determined using an event-by-event correction method derived by Grant.²⁴ The correction is based on a calculation of the component of the observed hadron jet momentum (Z_c) which is in the muon-neutrino plane and is perpendicular to the true hadron momentum direction. It is applied on an event-by-event basis, after the determination of a global constant which centers the average Z_c at zero. This global constant was determined separately for the charged-current and dilepton samples. It gave an average hadron-energy correction of $(23 \pm 3)\%$ [corresponding to a $(10 \pm 1)\%$ correction to the measured E_ν] for the charged-current events and an average hadron-energy correction of $(51 \pm 8)\%$ [$(27 \pm 5)\%$ in E_ν] for the dilepton events. This implies that, in the dilepton event sample, the missing neutrino from the semileptonic charm decay carries off $(19 \pm 5)\%$ of the hadron energy or $(13 \pm 4)\%$ of the incident neutrino energy. Comparable measurements in other experiments yield $(24 \pm 9)\%$ of the hadron energy¹⁵ and $(12 \pm 1)\%$ of the incident neutrino energy.⁶ The corrected neutrino energy distribution for the μ^-e^+ events is shown in Fig. 3(c).

The average positron momentum is much lower than the muon momentum. After correcting for background the ratio of their average momenta is $\langle P_{\mu^-} \rangle / \langle P_{e^+} \rangle = 6 \pm 1.5$. This implies that neutral-heavy-lepton decays cannot contribute significantly to the data sample.²⁵ If the e^+ comes from a charm decay then it should be associated with the hadron vertex. This can clearly be seen in the ϕ distributions (Fig. 4). Here ϕ is the angle between the projections of any two vectors in a plane normal to the neutrino direction. The projection of the momentum vector of the hadron system (all tracks except the μ^- and e^+ candidates) and of the e^+ track peaks backwards with respect to the muon while the distribution for the e^+ and the hadron vector is uniform.

The conventional kinematic variables are calculable once the muon energy (E_μ), the muon scattering angle (θ_μ), and the neutrino energy (E_ν) are known.

The measured distributions of the variables

$$Q^2 = 2E_\nu E_\mu (1 - \cos\theta_\mu),$$

$$x = Q^2 / 2m_p \nu,$$

$$y = \nu / E_\nu,$$

$$W = m_p^2 + 2m_p \nu - Q^2,$$

where $\nu = E_\nu - E_\mu$ and m_p is the proton mass, are shown in Fig. 5. Perhaps the most interesting distribution is x . In the GIM model charged-current neutrino interactions which do not produce charm particles occur predominantly by interactions on a d quark ($\nu d \rightarrow \mu^- u \dots$) with a strength proportional to $\cos^2\theta_C$ (where θ_C is the Cabibbo angle) or to a much lesser extent by interactions on a sea s quark ($\nu \bar{s} s \rightarrow \mu^- \bar{u} s$) with a strength proportional to $\sin^2\theta_C$ ($\sin^2\theta_C \approx 0.05$). Consequently the x distribution is essentially a d quark distribution. In this same model charmed particles are produced either by interactions on a

d quark ($\nu d \rightarrow \mu^- c \dots$) with a strength proportional to $\sin^2\theta_C$ or by interactions on a sea s quark ($\nu \bar{s} s \rightarrow \mu^- \bar{c} s \dots$) with a strength proportional to $\cos^2\theta_C$. Here the d quark contribution is suppressed by the Cabibbo mixing angle, and consequently one might expect a substantially different x distribution from that observed in charged-current interactions where few charm particles are produced. If one uses the d - and s -quark distributions determined in other experiments,²⁶ a fit to the measured x distribution gives a ratio of $s / (d \tan^2\theta_C) = 0.76 \pm 0.29$.

Since charm particles decay predominantly into strange particles (the $c \rightarrow s$ decay is ≈ 0.95 of all decays) when charm is produced from the d quark there will be approximately one strange particle per event, whereas in charm production from s quarks there will be approximately two strange particles. From the experimental ratio $s / d \tan^2\theta_C = 0.76 \pm 0.29$ one expects 1.38 ± 0.09 strange particles per μ^-e^+ event arising from the charm-production mechanism. This rate does not include strange particles which might arise from $s\bar{s}$ pairs which appear in the hadronization of the remaining target fragments. It should be noted that in either charm-production mechanism a c quark (not \bar{c}) is produced. Compared to noncharm events these charm events contain an extra c quark and sometimes an extra \bar{s} quark. Since the Λ contains an s quark, excess Λ 's must arise from the dominant c -quark decay ($c \rightarrow s$) and, consequently, most likely come from charmed-baryon decays. Both of these aspects of strange-particle production are discussed below.

B. Rate for μ^-e^+ production

The rate for opposite-sign dilepton production relative to normal charged-current production is quite sensitive to the momentum cut imposed on the second (e^+) lepton track. It is relatively insensitive to the momentum cut on the leading (μ^-) lepton since this cut is applied both to the dilepton and charged-current samples. The only cut imposed in this experiment is the requirement that the e^+ momentum be larger than 300 MeV/ c . The effect of this cut, while small, could affect the measured rate, especially at low neutrino energy.

The rate is calculated using a restricted fiducial volume containing 84% of the μ^-e^+ events. In determining this rate the following corrections for efficiencies have been used: (i) scanning efficiency $(75 \pm 5)\%$, (ii) identification of the e^+ $(85 \pm 5)\%$, (iii) loss due to obscured events $(10 \pm 5)\%$, and (iv) other miscellaneous losses such as a good single e^+ from the vertex appearing as a Dalitz pair because it is almost tangent to a leaving track $(5 \pm 5)\%$.

A total of 77 000 charged-current candidates are within the fiducial volume. After background subtraction this reduces to 61 600 charged-current events or an average of 0.47 charged-current events per picture in the fiducial volume.

The resulting dilepton rate is

$$R = \frac{\nu_\mu + N_e \rightarrow \mu^- + e^+ + \dots}{\nu_\mu + N_e \rightarrow \mu^- + \dots} = (0.52 \pm 0.09)\% .$$

There is no discernible high-energy threshold in the data. The effect of the 300-MeV cut on the e^+ momen-

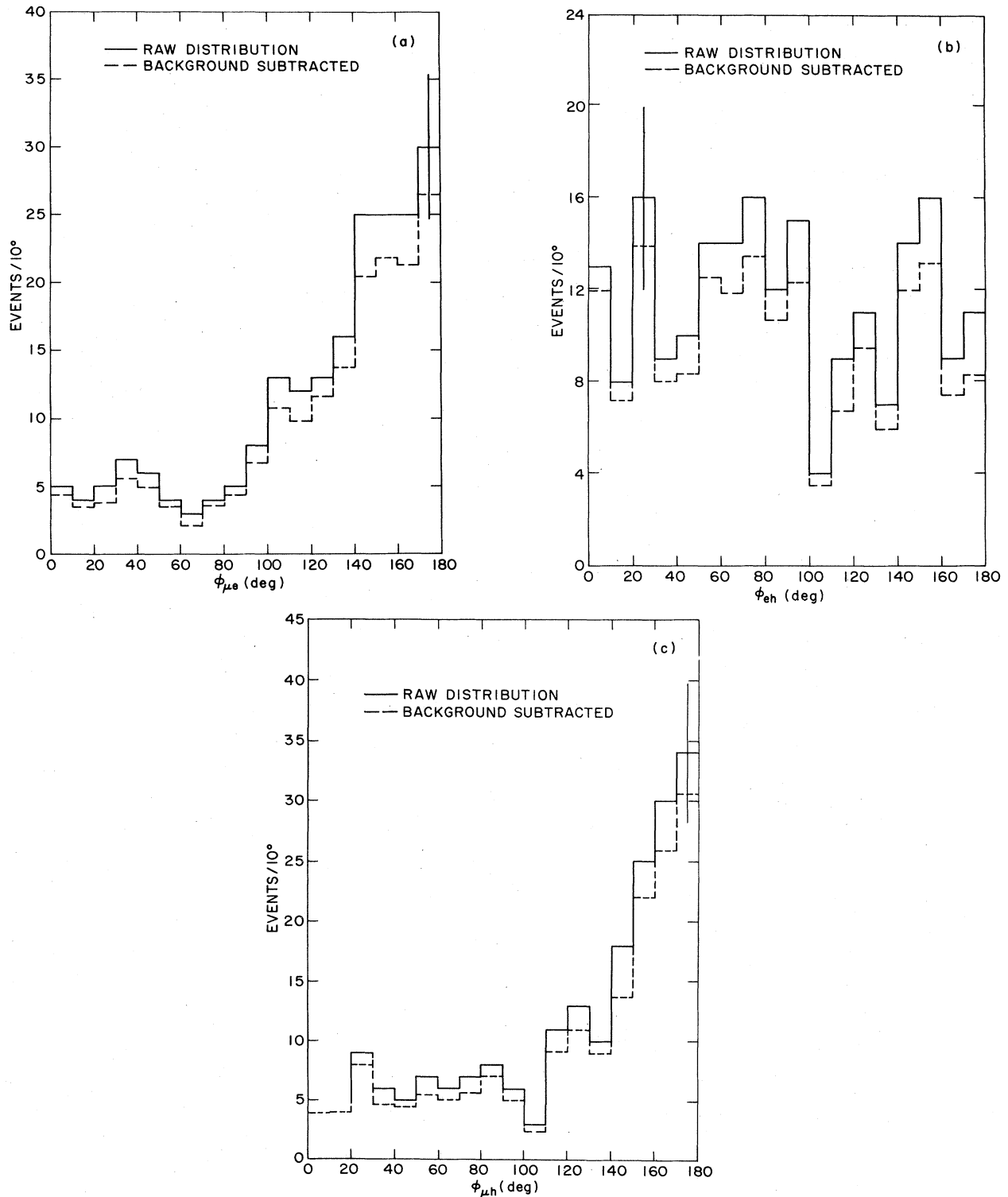


FIG. 4. ϕ distribution (a) between the muon and the positron, (b) between the positron and the hadron jet, and (c) between the muon and the hadron jet. The solid curve displays the raw distribution and the dashed curve is the background-subtracted distribution.

tum will be to preferentially decrease the rate at lower energies. Figure 6 shows the ratio of opposite-sign (μ^-l^+ ; $l=e,\mu$) events to normal charged-current events as a function of the incident neutrino energy for this experi-

ment and for other experiments in which the momentum cut applied to the second lepton is 300 MeV/c (Refs. 8 and 16) or for which the effect of the momentum cut has been corrected using a Monte Carlo simulation assuming

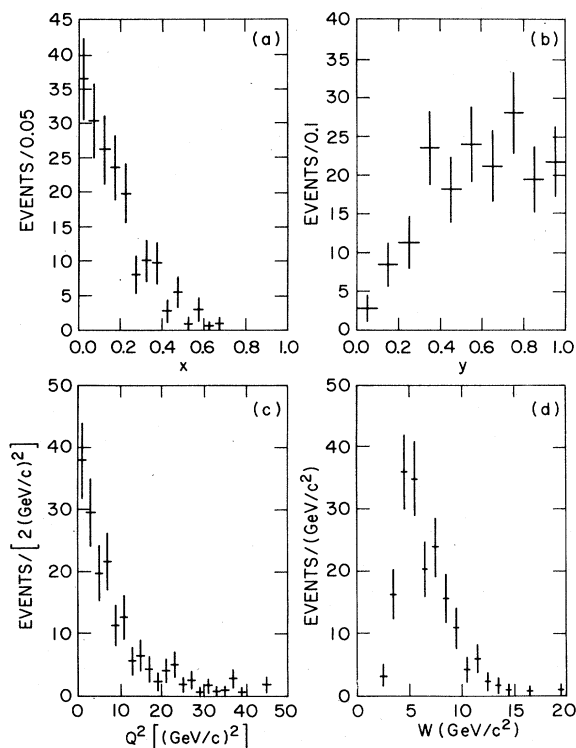


FIG. 5. Kinematic variables for opposite sign ($\mu^- e^+$) dilepton events (a) x , (b) y , (c) Q^2 , and (d) W .

charged- D -meson production.^{6,15} Counter experiments in general require both leptons ($\mu^- \mu^+$) to have momenta greater than 4 GeV/ c . If the same lepton momenta cuts are applied to this experiment, then the overall dilepton rate drops to $(0.16 \pm 0.03)\%$. The rate as a function of neutrino energy is shown in Fig. 7. As expected the effect of the momentum cuts is to sharply reduce the production rate at low energy. The equivalent distributions as measured in other high statistics experiments are also shown in Fig. 7. The agreement is quite good.

C. Strange-particle content

The $\mu^- e^+$ sample has been examined very carefully for possible associated V^0 's (i.e., neutral-strange-particle decays $K_S^0 \rightarrow \pi^+ \pi^-$, $\Lambda \rightarrow p \pi^-$, $\bar{\Lambda} \rightarrow \bar{p} \pi^+$). Kinematic fits to

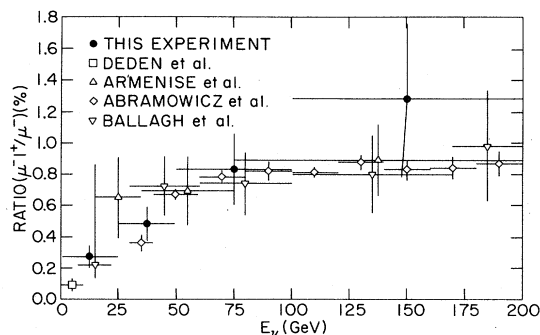


FIG. 6. Ratio of opposite-sign dilepton events per charged-current event as a function of the incident neutrino energy.

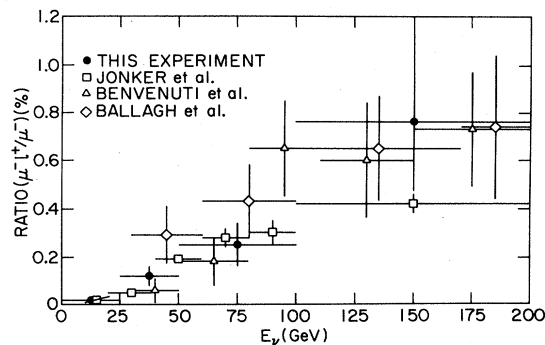


FIG. 7. Ratio of opposite-sign dilepton events per charged-current event as a function of the incident neutrino energy; all lepton momenta > 4.0 GeV/ c .

the primary vertex were attempted for all vee candidates. As a result of this fitting 58 V^0 's were obtained: 6 events have 2 V^0 's and 46 have a single V^0 . Of the 58 V^0 's, 34 fit to a single mass hypothesis; 25 are $K_S^0 \rightarrow \pi^+ \pi^-$, 8 are $\Lambda \rightarrow p \pi^-$, and 1 is $\bar{\Lambda} \rightarrow \bar{p} \pi^+$. The remaining 24 have ambiguous fits; 18 to Λ and K_S^0 and 6 to $\bar{\Lambda}$ and K_S^0 . It is possible to resolve the kinematically ambiguous solutions in a number of essentially equivalent ways. For example, if one assumes there are no genuine $\bar{\Lambda}$ produced, then the 6 ambiguous $K_S^0/\bar{\Lambda}$ imply that 6 of the 18 K_S^0/Λ ambiguous fits are K_S^0 . More precisely, if the overlap between the K_S^0 and Λ fits is the same as that between the K_S^0 and $\bar{\Lambda}$ fits, then it is possible to resolve the ambiguities using the observed unique fits. The ambiguous K_S^0/Λ fits are resolved into 4.3 K_S^0 and 13.7 Λ ; the ambiguous $K_S^0/\bar{\Lambda}$ are resolved into 4.3 K_S^0 and 1.7 $\bar{\Lambda}$. One can also consider the distribution of $\ln(P_+/P_-)$ where P_+ (P_-) is the momentum of the positive (negative) track of the V^0 (Fig. 8). For true $K_S^0 \rightarrow \pi^+ \pi^-$ decays this distribution should be symmetric. Therefore 7 of the ambiguous K_S^0/Λ events are true K_S^0 's. Alternatively one can look at the angle ($\cos^* \theta$) between the positive track and the K_S^0 direction in the K_S^0 rest system. If there were no ambiguities this distribution would be flat. Using the (≈ 5000) strange-particle decays in this experiment produced in normal charged-current interactions an event-by-event K_S^0/Λ ambiguity resolution (based on the relative K_S^0 and Λ fit probability) was determined so that the resulting $\cos^* \theta$ distribution for the selected K_S^0 was flat. If these kinematic-fit criteria are applied to the ambiguous V^0 's in the $\mu^- e^+$ sample 6 are selected as K_S^0 decays and the remaining 12 are Λ 's. In the strange-particle distributions discussed below the ambiguous events are resolved event by event using the relative-fit probabilities. After resolving ambiguities in the fits there are 37 $K_S^0 \rightarrow \pi^+ \pi^-$, 20 $\Lambda \rightarrow p \pi^-$, and 1 $\bar{\Lambda} \rightarrow \bar{p} \pi^+$.

The observation of 58 V^0 's in 249 $\mu^- e^+$ events is to be contrasted with the strange-particle content in charged-current events. If the same criteria as are used for the $\mu^- e^+$ events are applied, the rate for strange particles in charged-current events is 0.066 visible strange particles per event. Consequently, in 249 $\mu^- e^+$ events one would expect only 16 V^0 's but the $\mu^- e^+$ sample has 58 V^0 's. After resolving V^0 fit ambiguities in the charged-current data one would expect in 249 events to observe 9

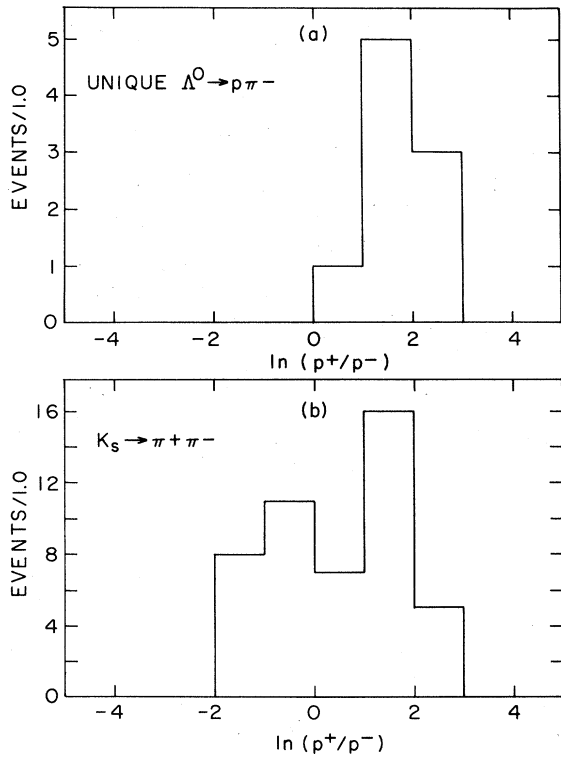


FIG. 8. Logarithmic momentum ratio for kinematically fitted neutral strange particles. (a) Unique $\Lambda \rightarrow p\pi^-$ fits; (b) $K_S^0 \rightarrow \pi^+\pi^-$ including ambiguous K_S^0/Λ fits.

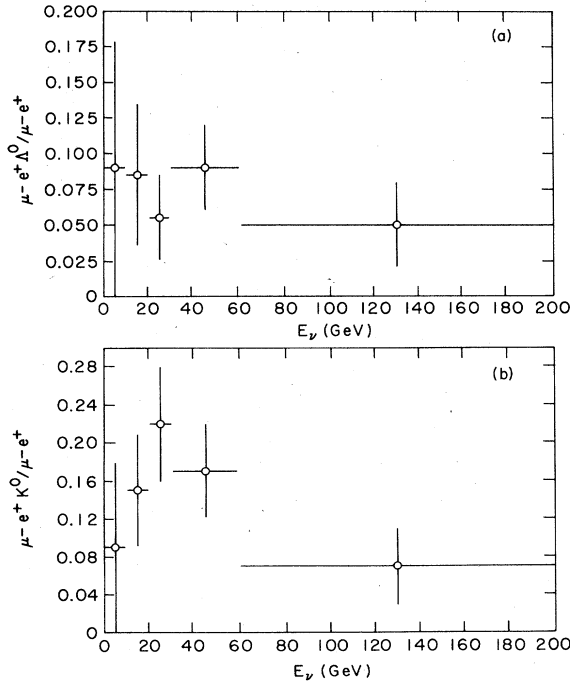


FIG. 9. Observed number of neutral-strange particles per opposite-sign dilepton event as a function of the incident neutrino energy for (a) Λ , and (b) K_S^0 .

$K_S^0 \rightarrow \pi^+\pi^-$, 7 $\Lambda \rightarrow p\pi^-$, and 1 $\bar{\Lambda} \rightarrow \bar{p}\pi^+$ decays from associated strange-particle production. The excess V^0 's in the μ^-e^+ events then are 28 K_S^0 , 13 Λ , and 0 $\bar{\Lambda}$. This excess of strange particles is a clear indication of charm production. It is difficult to precisely determine the number of strange particles per event due to charm production in the μ^-e^+ data sample. The observed strange particles in normal charged-current events arise both from associated strange-particle production ($s\bar{s}$ production) and from charm production ($d \rightarrow c \rightarrow s$) ($\bar{s}s \rightarrow \bar{s}c \rightarrow \bar{s}s$). If one assumes the average semileptonic decay for charm particles is $\approx 10\%$ then the total charm cross section at these energies is $\approx 5\%$ of the total charged-current cross section. The visible strange content in charged-current events due to nonleptonic charm decays would then be approximately 0.012 or 18% of the observed 0.066 strange particles per charged-current event. A lower limit on the number of strange particles per μ^-e^+ event due to charm production can be obtained by using the excess of 28 K_S^0 and 13 Λ calculated above. Correcting for the neutral decay modes of the K_S^0 and Λ and their detection efficiencies one finds that the excess number of K^0 's produced is 101 ± 25 and the excess number of Λ 's is 23 ± 9 . In other words, the excess number of neutral strange particles per μ^-e^+ event is (0.6 ± 0.15) . If the expected number of charged strange particles in the μ^-e^+ events is equal to the measured number of neutral strange particles (i.e., no. of $K^- =$ no. of \bar{K}^0 , etc.) the strange-particle excess in the sample is ≈ 1.2 . If one takes 0.054 (not 0.066) for the visible strange-particle rate per charged-current event and repeats the same calculation, a value of 1.3 strange particles per μ^-e^+ event is obtained. These estimates are clearly consistent with the charmed-model prediction from the x distribution that there should be 1.38 ± 0.09 strange particles per event.

Some features of the strange-particle content should be noted. The strange-particle content is not strongly dependent on the energy of the dilepton event (Fig. 9). The number of observed Λ 's is 20, whereas at most 7 are expected from associated production. Since Λ 's can only arise in the charm mechanism from c -quark decay this significant excess of Λ 's can only arise from the production of charmed baryons in the neutrino interactions. Second, the ratio of Λ to K^0 in the μ^-e^+ events is 0.23. This suggests that in the energy region of this experiment charmed-baryon production is significant. However it is not possible at this time to determine the charmed-baryon-to-charmed-meson production ratio since the relevant branching ratios, such as $B(\Lambda_c \rightarrow K^0 \dots)$, are not well established.

D. Effective-mass distributions

Since it is clear that most of the V^0 in the μ^-e^+ events are associated with charm production, it is interesting to examine effective-mass distributions for possible strange-particle resonances in the charm decays.

The Λe^+ effective-mass distribution is shown in Fig. 10. As expected, most Λ are consistent with being from charm decays [$m(\Lambda e^+) < m(\Lambda_c^+)$]. It is interesting to note that almost all the events with $P_{e^+} > 4$ GeV/c have

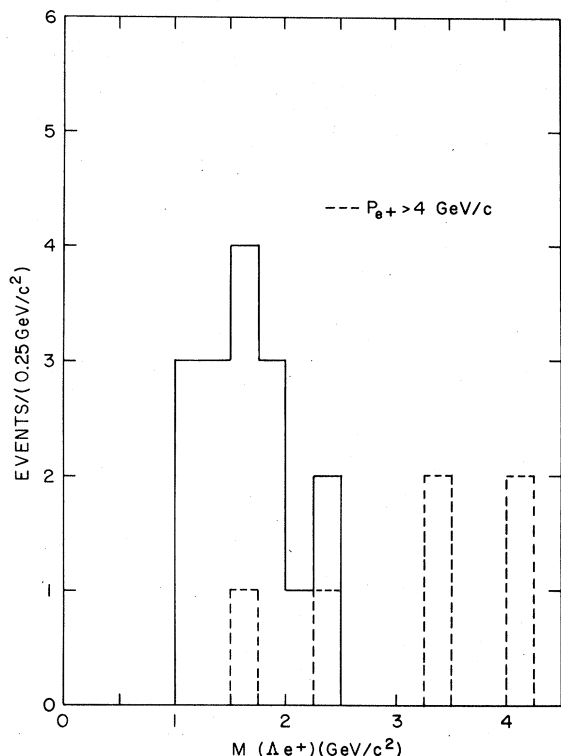


FIG. 10. Invariant-mass distribution for Λ and e^+ . Solid curve displays all combinations; dashed curve those combinations in which $P_e^+ > 4.0$ GeV/c.

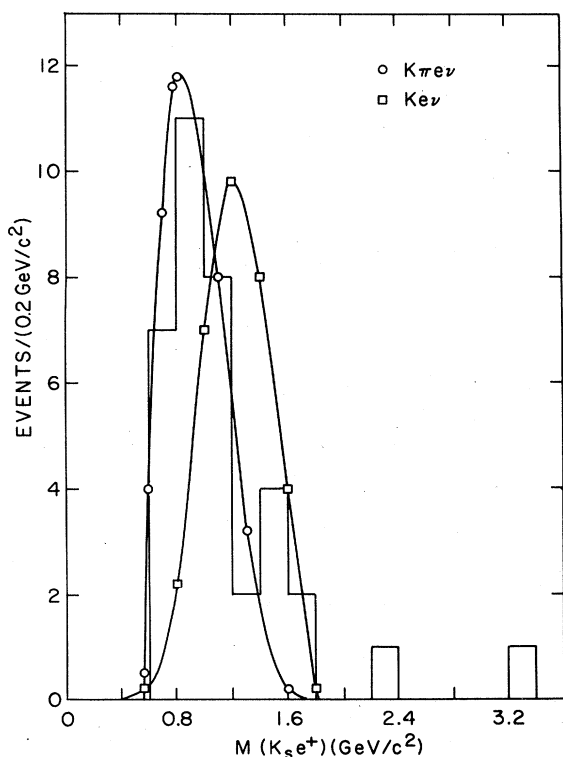


FIG. 11. Invariant-mass distributions for K_S^0 and e^+ . The lines represent the expected invariant-mass distributions for three- and four-body D decays.

effective masses larger than the Λ_c^+ mass. Since this is not true for meson decays as will be discussed below, one suspects then the electrons from charmed-baryon decays are softer than from charmed-meson decays. This effect is implicit in the results in bubble-chamber studies of $\mu^- \mu^+$ production where there is a high-lepton-momentum cut ($P_\mu > 4$ GeV/c) and where no excess Λ production is observed.¹⁵

The $K^0 e^+$ effective-mass distribution (Fig. 11) is clearly consistent with charmed- D -meson decays. It should be noted, however, that $\approx 25\%$ of the K^0 are either from associated strange-particle production or charmed-baryon decays. The shape of the distribution indicates a dominance of four-body D decays. It is not possible to distinguish here between $K^* e \nu$ and $K \pi e \nu$ decays. The apparent lack of a significant three-body decay contribution is not too surprising. Only the $D^+ \rightarrow K_S^0 e^+ \nu$ three-body decay can contribute ($D^0 \rightarrow K^- e^+ \nu$ has no K^0) while both D^0 and D^+ contribute to four-body decay.

Effective-mass distributions for events with $m(K\pi e) < 1.85$ GeV/c are shown in Fig. 12.

VI. CONCLUSION

It has been clear for some time that the opposite-sign dileptons observed in neutrino interactions are predom-

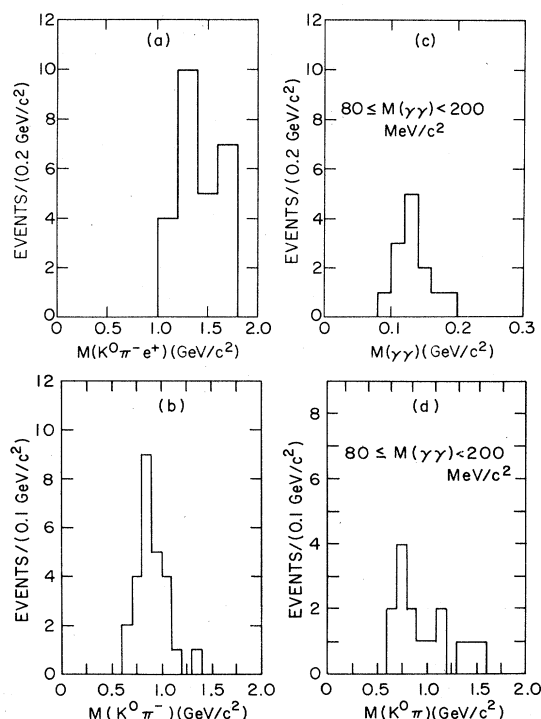


FIG. 12. Invariant-mass distributions for dilepton events where the $K\pi e$ effective mass is less than the D mass. (a) Invariant-mass distribution for $K^0 \pi^- e^+$. (b) Invariant- $K^0 \pi^-$ -mass distribution for events with $m(K^0 \pi^- e^+) < 1.86$ GeV/c². (c) Invariant- $\gamma\gamma$ -mass distribution for events with $m(K^0 \pi^0 e^+) < 1.86$ GeV/c² and $80 \leq m(\gamma\gamma) \leq 200$ MeV/c². (d) Invariant- $K^0 \pi^0$ -mass distribution for events with $m(K^0 \pi^0 e^+) < 1.8$ GeV/c² and $80 \leq m(\gamma\gamma) \leq 200$ MeV/c².

inantly the result of the semileptonic decay of produced charm particles. However the details of charm production are still unclear. High-statistics counter experiments yield good information on the relative contribution of sea-quark and valence-quark interactions to the rate. The major contribution of the present experiment lies in its ability to study the details of the final state and in the measurement of the excitation curve with minimal cuts on the lepton momenta. The rate of strange-particle production is quite consistent with that expected from charm production with the admixture of sea-quark and valence-quark production determined from the x distribution. The significant excess of strange baryons (Λ) established that charm baryons are being produced. In addition from the Λ/K_S^0 ratio of ≈ 0.23 it is clear that charmed-baryon production is significant at these energies. However with present data it is difficult to understand completely all the details of charm production by neutrinos.

A final data-taking run on this experiment is now being analyzed. This will more than double the present statistics. The new data was taken using the external muon identifier (EMI) with the 15-ft bubble chamber and this will greatly reduce the hadron-punchthrough background, which is a serious problem in the present analysis. Since the event rate per picture was lower on average in this last run it will afford a good test for possible scanning or analysis biases in the original film. It is expected that this new data will contribute significantly to our understanding of the final states in opposite-sign dilepton events.

ACKNOWLEDGMENT

This research has been supported in part by the U.S. Department of Energy under Contract No. DE-AC02-76CH00016.

*Present address: CERN, CH-1211 Geneva 23, Switzerland.

†Deceased.

‡Present address: Bell Laboratories, Murray Hill, NJ.

§Present address: Rutgers University, New Brunswick, NJ.

**Present address: Heidelberg University, Heidelberg, Federal Republic of Germany.

¹A. Benvenuti *et al.*, Phys. Rev. Lett. **34**, 419 (1975).

²A. Benvenuti *et al.*, Phys. Rev. Lett. **35**, 1199 (1975).

³B. C. Barish *et al.*, Phys. Rev. Lett. **36**, 939 (1976).

⁴A. Benvenuti *et al.*, Phys. Rev. Lett. **41**, 1204 (1978).

⁵M. Jonker *et al.*, Phys. Lett. **107B**, 241 (1981).

⁶H. Abramowicz *et al.*, Z. Phys. C **15**, 19 (1982).

⁷A. Benvenuti *et al.*, Phys. Rev. Lett. **35**, 1249 (1975).

⁸H. Deden *et al.*, Phys. Lett. **67B**, 474 (1977).

⁹P. Bosetti *et al.*, Phys. Rev. Lett. **38**, 1248 (1977).

¹⁰H. C. Ballagh *et al.*, Phys. Rev. Lett. **39**, 1650 (1977).

¹¹P. C. Bosetti *et al.*, Phys. Lett. **73B**, 380 (1978).

¹²O. Erriquez *et al.*, Phys. Lett. **77B**, 227 (1978).

¹³D. S. Baranov *et al.*, Phys. Lett. **81B**, 261 (1979).

¹⁴J. P. Berge *et al.*, Phys. Lett. **81B**, 89 (1979).

¹⁵N. Armenise *et al.*, Phys. Lett. **86B**, 115 (1979).

¹⁶H. C. Ballagh *et al.*, Phys. Rev. D **21**, 569 (1980).

¹⁷N. Armenise *et al.*, Phys. Lett. **94B**, 527 (1980).

¹⁸H. C. Ballagh *et al.*, Phys. Rev. D **24**, 7 (1981).

¹⁹P. Marage *et al.*, Z. Phys. C **21**, 307 (1984).

²⁰S. L. Glashow, J. Iliopoulos, and L. Maiani, Phys. Rev. D **2**, 1285 (1970).

²¹An analysis based on the first data sample from the experiment was published: C. Baltay *et al.*, Phys. Rev. Lett. **39**, 62 (1977).

²²A. M. Cnops *et al.*, in *Neutrino '79*, proceedings of the International Conference on Neutrinos, Weak Interactions, and Cosmology, Bergen, Norway, 1979, edited by A. Haatuft and C. Jarlskog (University of Bergen, Bergen, 1980).

²³From an examination of low-energy electrons it was determined that e^\pm tracks with energy $E > 5$ MeV could be reliably identified on the scanning table.

²⁴A. Grant, Nucl. Instrum. Methods **131**, 167 (1975).

²⁵A. Pais and S. B. Treiman, Phys. Rev. Lett. **35**, 1206 (1975).

²⁶The valence- and sea- x distributions used are $\sqrt{x}(1-x)^{3.5}$ and $(1-x)^7$, respectively. They are taken from Ref. 6 above and were determined in an analysis of single-muon data from the same experiment (Ref. 10 therein).